Sources and sinks of ozone in savanna and forest areas during EXPRESSO: Airborne turbulent flux measurements

B. Cros, Claire Delon, C. Affre, T. Marion, A. Druilhet, P. Perros, A. Lopez

JOURNAL OF GEOPHYSICAL RESEARCH, VOL. 105, NO. D24, PAGES 29,347-29,358, DECEMBER 27, 2000

Sources and sinks of ozone in savanna and forest areas during EXPRESSO: Airborne turbulent flux measurements

B. Cros,[1] C. Delon,[1] C. Affre,[1] T. Marion,[2] A. Druilhet,[1] P.E. Perros,[2] and A. Lopez[1]

Abstract. An airborne study of ozone concentrations and fluxes in the lower layers of the atmosphere was conducted over the Central African Republic (CAR) and northern Congo in November/December 1996, within the framework of the Experiment of Regional Sources and Sinks of Oxidants (EXPRESSO). The first 4 km of the atmosphere above savanna, rain forest, and the transitional area between them, were investigated with the French research aircraft Avion de Recherche Atmosphérique et de Télédétection (ARAT). Turbulent fluxes and deposition velocities of ozone were determined using the Eddy Correlation (EC) method. A specific methodology was developed to obtain accurate airborne turbulent flux measurements. This methodology is linked to the turbulence stationarity. The average values of ozone fluxes and ozone deposition velocities in the Atmospheric Boundary Layer (ABL) increase appreciably from savanna to forest. Near the ground, the ozone fluxes range between -0.115 +/-0.073 ppbv m/s above savanna and -0.350 +/- 0.115 ppbv m/s above forest; for the deposition, the ranges are 0.0042 +/- 0.0018 m/s and 0.015 +/- 0.004 m/s. A simple empirical relationship between deposition velocity and Leaf Area Index (LAI) is proposed, giving an estimation of the deposition velocity for a whole latitudinal band. Vertical inputs of ozone to the ABL are estimated according to entrainment fluxes. The role of advection is neglected for horizontal transport of ozone in the ABL. The photochemical ozone production is deduced from the photo-stationary state deviation, and compared to the net ozone increase in the ABL during the flights performed above the forest. A tentative ozone budget based on the aircraft measurements is proposed in the ABL of the rain forest. Around noon, the photochemical production dominates with a net production of about 10 ppbv/h.

1. Introduction

Previous measurements in the African tropics through remote sensing and in situ observations [*Fishman et al.*,1986; *Cros et al.*, 1988; *Marenco et al.*, 1990; *Lacaux et al.*, 1996] have shown high emissions of trace gases from biomass burning. These emissions involve a widespread pollution of the troposphere [*Fishman et al.*, 1991], and one of the most dramatic features of this pollution is the seasonal enhancement of tropospheric ozone on the West Coast of southern Africa [*Fishman et al.*, 1990]. The recent Transport and Atmospheric Chemistry Near the Equator-Atlantic (TRACE-A) experiment [*Fishman et al.*, 1996] has shown that the presence of fires in southern Africa was not sufficient to generate the ozone maximum observed in the upper troposphere. The ozone accumulation in this zone could result from a combination of complex mechanisms of atmospheric chemistry and meteorological processes. The yearly amounts of biomass burnt in the northern African tropics are similar to those of the southern African tropics [*Lefeivre*, 1993]. However, the atmospheric consequences of biomass burning, particularly for tropospheric ozone, seem to be appreciably different between northern and southern African tropics as shown by satellite data from the Total Ozone Mapping Spectrometer (TOMS) [*Fishman et al.*, 1992]. In addition, Dynamique et Chimie de l'Atmosphère en Forêt Equatoriale (DECAFE) experiments have shown that effluents from northern African savanna fires can reach the equatorial rain forest (or tropical rain forest) and react with biogenic compounds emitted by this forest [*Andreae et al.*, 1992; *Cachier and Ducret*, 1991]. The specific chemistry involved under these conditions has a decisive effect on the evolution of the majority of the emitted compounds.

One of the primary goals of EXPRESSO [*Delmas et al.*, 1999] was to better quantify the exchange fluxes of reactive trace gases between the biosphere and the atmosphere in the northern African tropics, and to analyze the horizontal interactions at the transition between savanna and rain forest. The question addressed in this paper is whether the rain forest and the savanna act as net sources or sinks of oxidants such as O_3, and how these sources/sinks may be quantified over the whole investigated region. This study is also a first step in the evaluation of the regional influence of these sources and sinks.

Biosphere-atmosphere exchanges are governed by surface fluxes of energy and trace compounds. Temporal evolution of such fluxes may be monitored from fixed point measurements, but their spatial variability at regional scale require airborne measurements.

At the top of the ABL, exchanges with the upper layer determine the impact of emissions on regional atmospheric

[1]Laboratoire d'Aérologie, Unité Mixte de Recherche 5560, Centre National de la Recherche Scientifique/Université Paul Sabatier, Observatoire Midi Pyrénées, Toulouse, France.
[2]Laboratoire Interuniversitaire des Systèmes Atmosphériques, Unité Mixte de Recherche 7583, Centre National de la Recherche Scientifique/Université Paris 12, Créteil, France.

Paper number 2000JD900451.
0148-0227/00/2000JD900451$09.00

chemistry. Measurements of ozone fluxes near the surface help to understand the mechanisms for surface removal of ozone and eventually to identify the potential for biological effects on ozone deposition. During the EXPRESSO campaign a tentative budget of ozone in the ABL was established from the determination of ozone fluxes, both near the ground and near the top of the ABL. Because of measurement and logistic difficulties, very little quantitative information is available on the exchange rates within the interior of the ABLs of the studied area.

In this paper, our interest is focussed on deposition, input and formation of ozone in the ABL above savanna, rain forest, and transitional areas during the EXPRESSO campaign, which took place in November/December 1996 in Central African Republic (CAR) and northern Congo. Ozone flux measurements were conducted onboard the Fokker 27 ARAT, equipped for Eddy Correlation (EC) measurements of thermodynamic parameters (heat, water and momentum) and ozone concentrations. First, the deposition velocity V_d is estimated over the forest, and an empirical relationship between V_d and the Leaf Area Index (LAI) is proposed. Second, a tentative ozone budget in the ABL of the rain forest is proposed. To this end, vertical contributions are estimated from entrainment fluxes, and photochemical ozone production is deduced from the photo-stationary state.

2. The Experimental Area

2.1. Meteorological Characteristics

The climate in northern Africa is regulated by the Intertropical Convergence Zone (ITCZ), a zone of low pressures between converging winds from opposite hemispheres: the dry northeasterly continental trade wind, the so-called Harmattan flow, and the moist monsoon originating in the South Atlantic Ocean. The ITCZ extends over large areas of rain forest. This zone, sometimes ill-defined, can be detected by wind profiles, dew point, and temperature discontinuities in the first kilometers of the atmosphere. Its latitudinal position is linked to the apparent motion of the Sun, and its ground trace moves from about 20°N in July, to its most southerly position about 4°-5°N in December. Its seasonal shift determines the rain patterns and involves the alternation between wet and dry (i.e., burning or fire) seasons. In the EXPRESSO area (southern CAR and northern Congo) the dry season lasts from November to March (ground trace of ITCZ: from 4° to 8°N), and the wet season lasts from April to October (ground trace of the ITCZ: from 8° to 20°N). Figure 1 shows the evolution of rainfall patterns throughout the year (data taken in 1992-1993). The field campaign lasted from November 21 to December 2, at the transition between wet and dry seasons, which involved a strong instability of the layers of the lower troposphere. During EXPRESSO the monsoon dominated the flow in the ABL which rarely exceeded 1000 m in thickness. However, during short periods, (November 29 and 30) the monsoon flow gave way to the Harmattan flow in the ABL because of the proximity of the ITCZ at this period of transition. During daytime the monsoon layer can be assimilated to the mixed layer (or ABL), limited at the top by a strong temperature inversion and a humidity gradient. During the first week of the campaign, the ground trace of the ITCZ was located around 7°-8°N, and moved southward to 5°N at the end of the campaign. As a consequence, meteorological features in the savanna and the forest during the campaign became complicated by the proximity of the ITCZ.

2.2. Fire Distribution

Pyrogenic emissions in the northern African tropics occur mainly in the savanna zone, between 5° and 15°N. Generally, the fire period (corresponding to the dry season) begins in early November, peaks in January, and ends in February/March [*Cahoon et al.*, 1992]. This scenario depends on climatic conditions and may undergo important year to year variations. During this period the wide band of fires sweeps across savanna zones from the south of the Sahara desert to the borders of the equatorial rain forest. Between the Sahara desert and the rain forest several climatic domains exist, defined by distinct patterns: annual rainfall, relative

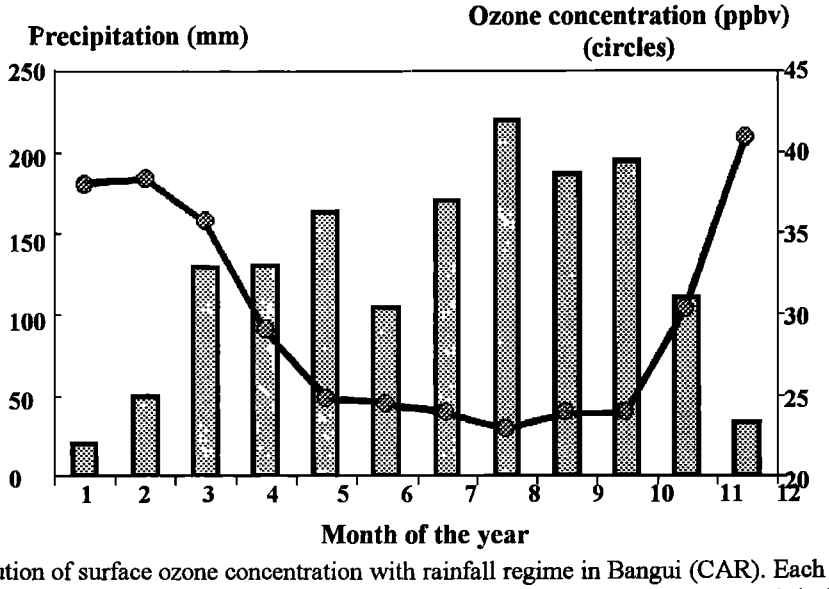

Figure 1. Evolution of surface ozone concentration with rainfall regime in Bangui (CAR). Each point (circle) represents the monthly mean value of daily maximum surface ozone mixing ratio measured during 1992 and 1993. Vertical bars give the precipitation in millimeters.

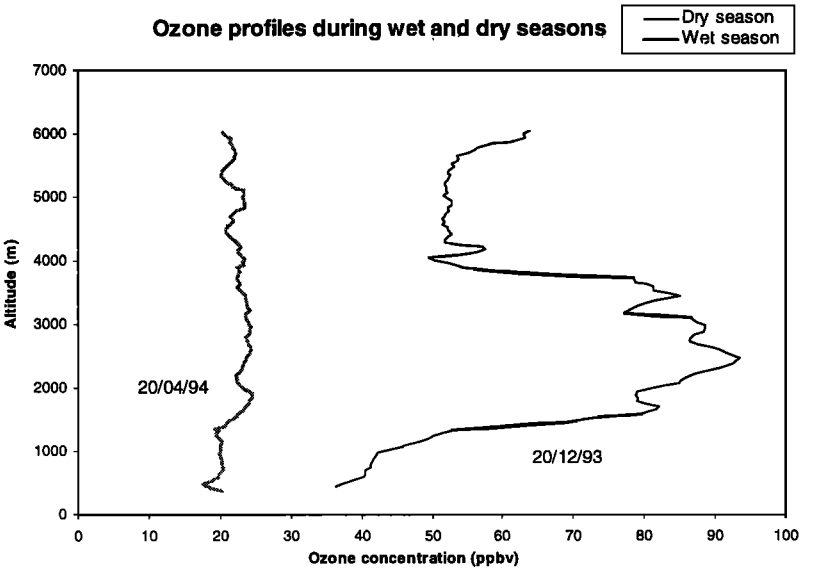

Figure 2. Typical vertical ozone profiles (0-5000 m) over Bangui (CAR) during the wet season (April 1994) and the dry season (December 1993). Ozone data were recorded between 1100 and 1400 UT.

humidity, average temperature, and relative length of the seasons. These patterns are laid out in parallel latitudinal belts [*Leroux*, 1980]. The associated climatic conditions determine the temporal and spatial evolution of savanna fires. In the northern African tropics the fire front may be considered as a wide strip moving from the Sahel to the Equatorial forest during the dry season (between November and February) as shown by *Grégoire et al.* [1999]. In the EXPRESSO zone (1.3 10^6 km^2) the number of daily detected fires varied between 1200 and 3760 for the period November 19 to 28. These fires were mainly located in the north CAR near the borders of Sudan and Chad. Some of them were located very close to the forest zone, and their influence on the chemical composition of the atmosphere was quite important.

2.3. Seasonal and Vertical Ozone Distributions

To choose the best period for an important field experiment in CAR, preliminary studies were conducted in Bangui (4°N, 18°E). Surface ozone measurements were performed between January 1992 and December 1993 using UV absorption instrumentation, and 16 ozone sondes were launched between December 1993 and April 1994. Figure 1 gives the evolution

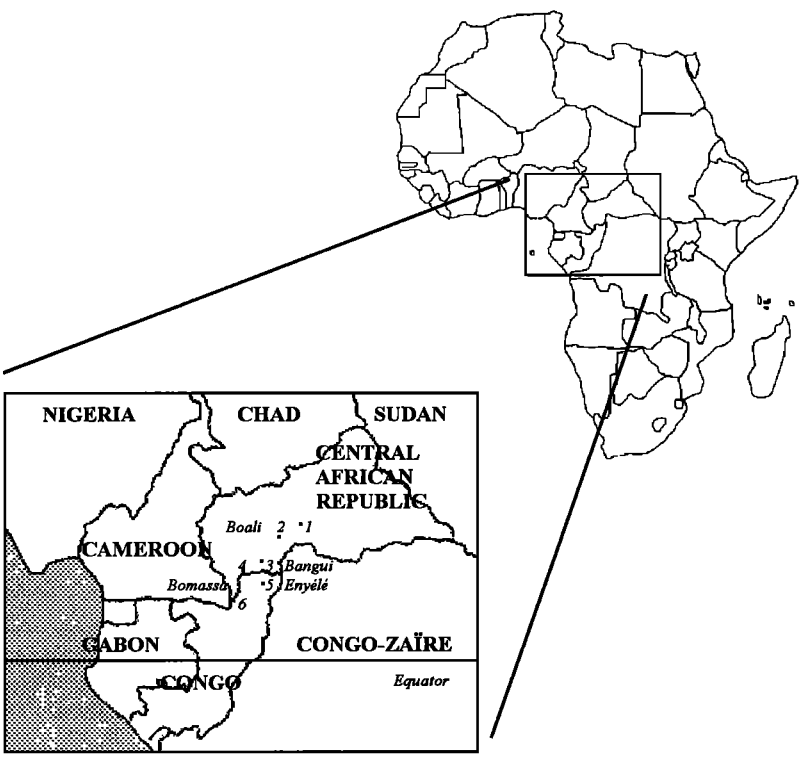

Figure 3. Map of central Africa showing the area investigated and the studied sites (1, 2, woodland savanna; 3, transition woodland; 4, secondary forest; 5, 6, primary forest) during the EXPRESSO campaign.

Table 1. Numbers, Dates, Hours and Location of the Flights Performed During the EXPRESSO Experiment

Flight	Beginning and End of the Flight, UT	Dates	Description	Type of Ecosystem
43	1223-1409	Nov. 21	test flight above Bangui savanna	
44	0924-1118	Nov. 22	Boali savanna flux measurements	savanna 2
45	0934-1138	Nov. 24	Boali savanna flux measurements	savanna 2
46	0927-1142	Nov. 25	Enyélé rain forest flux measurements	rain forest
47	0930-1145	Nov. 26	Enyélé rain forest flux measurements	rain forest
48	1057-1319	Nov. 27	gradient study in the Harmattan layer	savanna 1
49	0953-1156	Nov. 28	Enyélé rain forest flux measurements	rain forest
50	0922-1139	Nov. 29	transect above Bomassa rain forest	no low level legs
51	0958-1216	Nov. 30	Boali savanna flux measurements	savanna 2
52	0929-1151	Dec. 1	Enyélé rain forest flux measurements	rain forest
53	0836-1037	Dec. 2	savanna-forest interface	transitional woodland

of monthly mean values of daily maximum surface ozone mixing ratio, calculated from the 2-year measurement period (1992-1993). There is a strong increase in surface ozone during the dry season: the mixing ratio reaches 22 ppbv in October (end of the wet season), and 41 ppbv in December. November can be defined as a transition period between the two seasons, during which the rainfall decreases strongly in Bangui (from 190 mm in October to 25 mm in December). The EXPRESSO campaign was conducted at this exact period of the year. In rain forest zones, south of the ITCZ, the alternation of seasons is far less marked in rainfall patterns than in savanna zones. The strong seasonal cycle of surface ozone in Bangui shown in Figure 1 has also been observed in other sites of tropical Africa influenced by biomass burning.

Our data were recorded at the beginning of the dry season, when the ozone increases considerably. During this season in the Harmattan layer (HL, layer where the Harmattan flow blows), ozone mixing ratios, obtained from ozone soundings, are typically 70-80 ppbv, with maximum values up to 95 ppbv (Figure 2). The rate of ozone production increases from the wet to the dry season [*Cros et al.*, 1996]. The ozone increase in Dobson Units (DU) is about 35% in the HL (from 1.5 to 4 km), and about 12% in the ABL beneath.

2.4. Sampling Area for EXPRESSO (November-December 1996)

Airborne flux measurements of ozone at different levels and vertical ozone profiles were conducted along a 500 km transect, from the savanna of CAR to the tropical forest of the Congo. The direction of this transect is approximately the direction of the Harmattan wind, which transports the biomass burning effluents in the lower troposphere. To facilitate the airborne flux measurements, the different measurement areas were selected on the basis of the homogeneity of the ecosystems: woodland savannas, savanna-forest transition, secondary, and primary forests. Six areas located between 2°10'N and 5°50'N were investigated during the EXPRESSO campaign, as shown in Figure 3. The ARAT flew 11 missions (flights 43 to 53, Table 1) from its ground base in Bangui (CAR), during the twelve operational days. The flights were carried out over the savanna near Boali and Sibut (sites 1 and 2), over the transitional area near M'Baïki and Ngotto (sites 3 and 4), and over the rain forest near Bomassa and Enyele (sites 5 and 6). The coordinates are given in Table 2. The flight plans were designed to study surface fluxes above the canopy of these different vegetal covers, and fluxes at the top of the boundary layer.

3. Ozone Turbulent Fluxes and Deposition Velocities

3.1. Measurement Techniques

Vertical fluxes of ozone (Φ) were measured in the atmospheric surface and boundary layers by the EC method. The EC method is based on the computation of covariances of the fluctuations of the vertical wind component (W') and the

Table 2. Coordinates and Names of the Different Types of Ecosystems

Name of the Site	Coordinates, deg	Type of Ecosystem
Bangui	4.22°N, 18°35E	
Boali	4°48N, 18°07E	savanna 1
Sibut	5°44N, 19°05E	savanna 2
M'Baïki	3°53N, 18°00E	transitional woodland
Ngotto	4°08N, 17°15E	secondary forest
Bomassa	2°13N, 16°23E	primary rain forest
Enyélé	2°49N, 18°06E	primary rain forest
Ouesso	1°37N, 16°04E	primary rain forest

ozone concentration (O_3') [*Weseley et al.*, 1982]. The ozone flux is given by

$$\Phi = \overline{W'O_3'} = \frac{1}{T}\int_0^T W'(t)O_3'(t)dt \quad (1)$$

The primed symbols denote the fluctuations of the corresponding variables, and overbars refer to averages over successive time interval. The averaging time of flux measurements is about 5 min and corresponds to a path length of 50-60 km, with an aircraft speed around 100 m/s. This method requires the use of fast-response sensors. The OSG2 chemiluminescent sensor was used for ozone measurements, and is described by *Günsten et al.* [1992] and *Günsten and Heinrich* [1996]. This sensor has a response time faster than 0.1s and a detection threshold of 50 pptv. Its calibration was checked by comparison with a more slowly responding ozone sensor, a commercial UV absorption instrument (Thermo-Electron model 49), submitted to pressure and temperature controls. This last analyzer was also used for ambient ozone measurements.

Aircraft-based measurements of ozone fluxes by the EC method [*Lenschow et al.*, 1981; *Affre et al.*, 1999a] involve the following: (1) simultaneous measurements of ozone and wind fluctuations, (2) assessment of ozone flux accuracy, and (3) calibration of ozone fluctuations. To minimize the flow distortion, wind fluctuation sensors are located on the nose boom of the aircraft, far from the OSG2 ozone sensor (located in the cabin). As a consequence, ozone measurements are delayed compared with wind fluctuation measurements, and the time lag must be estimated to correct its effects.

We evaluate this time lag by studying the lagged correlation between temporal series of ozone fluctuations measured with the ozone sensor in the cabin, and humidity fluctuations measured with the «Lyman α» hygrometer on the boom, near the wind sensor. Ozone and humidity fluctuations are strongly anticorrelated in the lower troposphere of this region (Figure 4a). The process explaining the anticorrelation can be described as follows: dry deposition processes over a dense vegetation typically involve a downward flux of ozone molecules in the ABL. At ground level the evapo-transpiration provides an upward flux of humidity, and at the top of the ABL exchanges with the drier and enriched ozone upper layer intensify the downward ozone fluxes, and increase the anticorrelation. The absolute value of the correlation coefficient between ozone and humidity fluctuations (Figure 4b) is maximum when the measurements are performed in the same air parcel. The position of this maximum gives a good estimation of the time lag between ozone and humidity measurements. This value is constant and

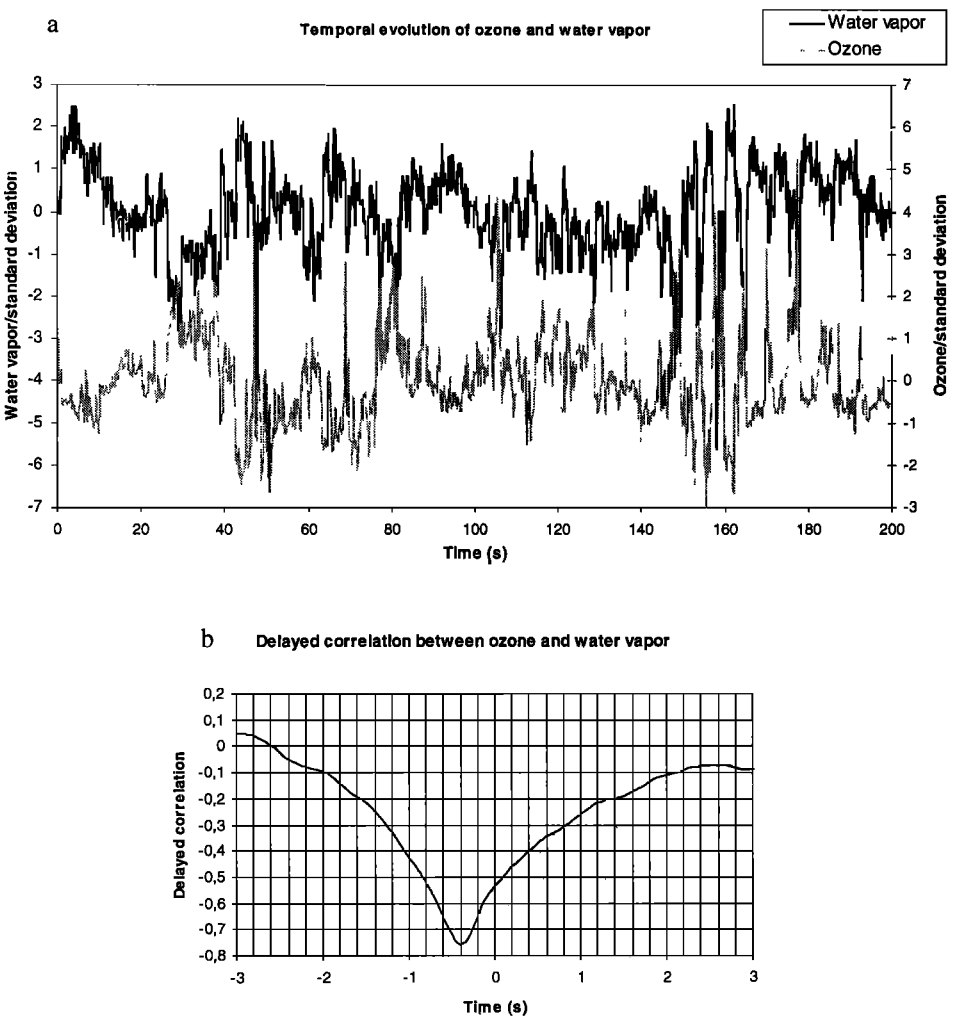

Figure 4. (a) Temporal series (one point every 1/16 s) of ozone (measured in the vein) and water vapor (measured in the boom); (b) Correlation function between ozone and water vapor measurements.

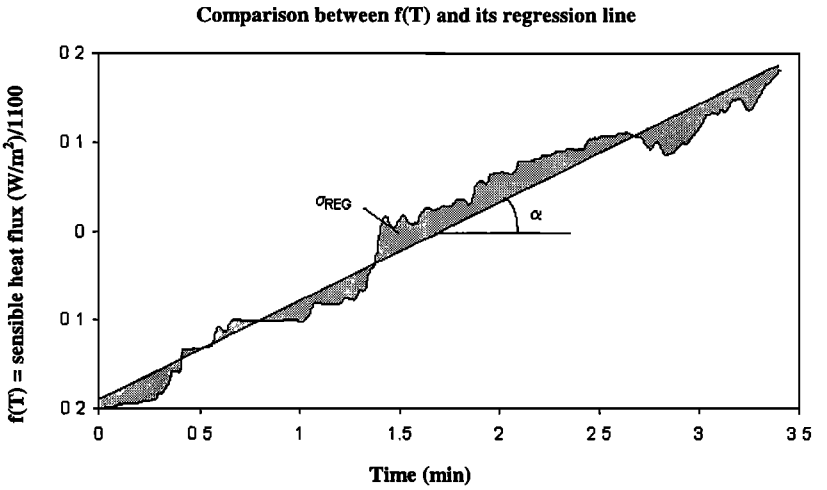

Figure 5. Correlation coefficient between f(T) (sensible heat flux, in W/m^2, divided by 1100) and its regression line. $\alpha = 0.378$ is the slope of the regression line. The shaded areas correspond to $\sigma_{REG} = 0.0427$, standard deviation between f(T) and its regression line. α/σ_{REG} = 12% gives the accuracy of the flux calculation.

equal to 0.4 s for all flights, at each level, when the altitude and the velocity of the plane (100 m/s) are constant. The absolute mean value of the correlation coefficient between ozone and humidity measurements during the campaign is 0.82, with a standard deviation of 0.14.

A Teflon tube (1/4 inch) allowed the sampled air to be driven from the boom to the O_3 sensor located in the cabin, and created an attenuation of high frequencies in the air vertical velocity. The result is an underestimation of ozone fluxes, assessed by comparing water vapor fluxes on the aircraft boom and in the inlet tube. This comparison gave a underestimation less than 12%. The theoretical explanation of the comparison between water vapor fluxes is not the purpose of this paper, and is given elsewhere by *Affre et al.* [1999a]. The major attenuation, (around 12%) having an effect on the ozone flux is due to its attenuation in the vein. The attenuation due to the time constant of the OSG2 (0.1s) can be considered as minor, and is not taken into account.

The comparison of the mean ozone concentrations $[O_3]_{ref}$ and $[O_3]_{OSG2}$, obtained with the slow (i.e., reference) and the fast ozone sensors, respectively, gives a calibration coefficient C, defined by

$$[O_3]_{ref} = C \times [O_3]_{OSG2}. \quad (2)$$

This coefficient gives the ozone flux Φ in a useful unit (ppbv m/s). C may vary from flight to flight, and may introduce an error of 1-5% in the flux measurement, depending on the flight. Turbulent vertical ozone fluxes are calculated with the EC method, according to equation (1). In calculating the flux by (1), one must make an assumption of stationarity. The function f(T) can be defined as follows:

$$f(T) = \int_0^T W'(t) O_3'(t) dt . \quad (3)$$

The evolution of f(T) determines the accuracy of the flux. Φ is well-determined when the derivative of f(T) does not depend on the integration time T (i.e., the calculation is accurate only if the turbulence is stationary). The closer the turbulence is to stationarity, the more linear is f(T), and the more accurate is the flux. This can be quantified by the correlation coefficient between f(T) and the linear regression line to f(T), that is the closest line to f(T) in the sense of linear regression. When the transfers are stationary, f(T) is linear and coincides with its linear regression line. When turbulent transfers are not stationary, f(T) is nonlinear, the linear regression line differs from f(T), and the evaluation of the flux is less accurate [*Affre et al.*, 1996].

The standard deviation between f(T) and its linear regression line is called σ_{REG}. *Affre et al.* [1999a, 1999b] use the ratio between σ_{REG} and α (the slope of the regression line), a good criterion of the stationarity of transfers. σ_{REG}/α is large (close to 100%) when the transfers are nonstationary. This criterion, expressed in percent, gives an estimate of errors in the flux calculation (Figure 5 and Table 3).

Table 3. Fluxes and Deposition Velocities of Ozone in the Surface Layer Over Different Sites Representing Savannas, Transitional Area, and Rain Forest in Central Africa [a]

	Altitude, m	Flux Φ_s, ppbv m/s	Deposition Velocity V_d, m/s	Stationarity Criterion SC, %
Savanna 1	185 (4)	-0.115±0.073	0.0042±0.0018	12
Savanna 2	70 (9)	-0.252±0.108	0.0068±0.0019	12
	240 (7)	-0.249±0.138	0.0081±0.0019	13
Transional area	90 (4)	-0.377±0.120	0.0100±0.0015	12
Forest	80 (8)	-0.349±0.115	0.0148±0.0042	7
	110 (11)	-0.354±0.0152	0.0147±0.0039	7
	190 (11)	-0.376±0.166	0.0154±0.0044	8

[a] Numbers in parenthesis give the leg number performed around the given altitude.

Finally, density corrections for air temperature fluctuations must be added to flux measurements of ozone as a result of the fact that density is not a conserved quantity. Heat and water vapor transfers induce a mean vertical mass flux, which is not taken into account in eddy correlation calculations. This correction, first applied by *Webb et al.* [1980] on water vapor and CO_2 measurements, can be expressed for ozone by the equation:

$$\Phi(O_3)_{corr} = \Phi(O_3)_{raw} + 0.85[O_3]_{ppbv}\,(0.649\ 10^{-6}\ \lambda E + 3.358\ 10^{-6}\ H) \quad (4)$$

where λ is the latent heat of vaporization, and where λE and H are the latent and sensible heat fluxes, respectively (in W m^{-2}). This correction is generally weak (around 4% in average).

3.2. Deposition Velocity

The ozone deposition velocity can be written as follows :

$$V_d = -\Phi(O_3)/\overline{X(O_3)} \quad (5)$$

where $X_{(O_3)}$ is the corresponding ozone mixing ratio. By convention, a downward flux is negative, so that V_d is positive for deposition.

During the campaign the deposition velocity V_d was deduced (for some flights) from EC measurements and from the mean ozone concentration. V_d is calculated from the fast-response ozone sensor assuming that ozone concentrations were accurate and that the time lag has been corrected:

$$V_d = \overline{w'O_3'}/[O_3]_{DSG2} \quad (6)$$

The transect investigated by the flights covers woodland savannas to rain (also called primary) forest. Savanna 1, in the northern part of the EXPRESSO area, is covered by woodland savanna Savanna 2, around Boali, west of Bangui, is also covered with woodland savanna but with higher grass and tree densities than in savanna 1. The primary forest is located near Enyele, 200 km south of Bangui, and at Bomassa, 350 km southwest of Bangui, both in Congo. Between Bangui and the primary forest, the aircraft flew over a transitional zone of degraded (or secondary) forest and small savanna. Table 3 summarizes the surface fluxes and deposition velocities based on EC measurements in the lower part of the ABL over these sites. Forest sites are not distinguished on Table 3 because they give similar results.

Generally, the turbulent functions are more stationary over forest than over savanna because the ground coverage is more homogeneous, and the fire perturbations weaker. The criterion α/σ_{REG}, defined at the end of part 3.1, is lower over forest (7-8%) than over savanna (12-13%), indicating a more precise flux measurement over forest.

Although ozone flux measurements over African tropical savanna areas are scarce, several studies have been conducted over rain forest. Cros et al. [1992a] estimated ozone fluxes in the mixed layer from tethered balloon measurements, using a gradient method. Similar values of ozone fluxes were observed in the northern Congo near the forest area investigated during EXPRESSO. The average flux during EXPRESSO was -0.32 +/- 0.11 ppbv m/s in the morning. In the central Amazon forest, vertical fluxes of O_3 measured by *Fan et al.* [1990] at the top of the canopy were about –0.115 ppbv m/s in average, a factor of 2 lower than our values. Corresponding deposition velocities (1.8 cm/s) were slightly higher than ours, but allow the conclusion that the forest investigated during EXPRESSO is close to the equatorial forest of the American continent. Indeed, Table 3 indicates a surface ozone flux of - 0.115 ppbv ms^{-1} over savanna 1, and quasi-constant ozone flux in the lowest layer of savanna 2 (-0.252 ppbv ms^{-1} at 70 m and -0.249 ppbv ms^{-1} at 240 m). We found also -0.376 ppbv ms^{-1} over rain forest at 190m. These results show that the ozone surface flux increases in absolute value from savanna (north of the EXPRESSO zone) to rain forest (south of the zone), with values ranging from -0.115 ppbv m/s to -0.35 ppbv m/s. The decrease of the deposition velocity V_d with latitude is regular, with values ranging from 0 4 cm/s for northern savanna to 1.5 cm/s for rain forest. They can be compared to values found over a coniferous forested area in Southwest of France (around 0 5 cm/s during the day [Carrara, 1998]), due to the turbulence intensity and to surface reactions (the principal component is the stomata opening), depending on biomass density, and therefore on LAI

To better understand the evolution of V_d with the landcover, we compared V_d to the Leaf Area Index (LAI) of each site. The LAI (ratio of the total leaf area to the area of the ground) was measured in central Africa during EXPRESSO by Klinger et al. [1998] during 1995 and 1996 along an 800 km transect from grassland savanna to primary forest. It appears, as shown in Figure 6, that there is a linear relation between V_d and LAI given by the following relation:

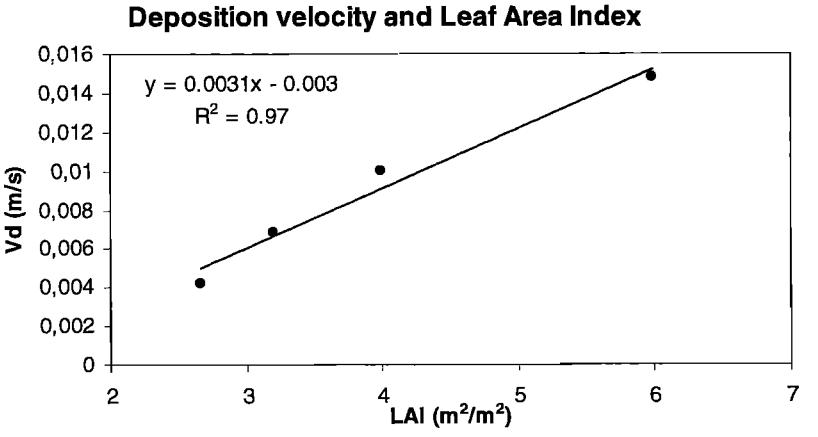

Figure 6. Linear regression between deposition velocity V_d and Leaf Area Index (LAI) for four different sites.

$$V_d = 3\times10^{-3}\,(\mathrm{LAI}-1) \quad (7)$$

where V_d is in m s^{-1} and LAI in m^2 of leaf per m^2 of ground.

To show that in our case, surface reactions are the essential cause for the spatial variability of ozone deposition, we use the following definition for V_d. In terms of resistances,

$$V_d = \frac{1}{r_a + r_b + r_c} \quad (8)$$

where r_a is the aerodynamic resistance, r_b is the laminar sublayer resistance, and r_c is the surface resistance. According to *Cieslik and Labatut* [1997],

$$r_a = \int_{z_0+d}^{z_M} \frac{dz}{K_H(z)} \quad (9)$$

where $K_H(z)$ is the vertical turbulent diffusion coefficient for scalars, z is the height, z_0 is the roughness length, z_M is the height of measurements, and d the displacement height. The parameters z_0 and K_H have been calculated during EXPRESSO by *Delon et al.* [2000]. They are 10m (z_0) and 21.9±8.7 m^2/s (K_H) above forest, 5m (z_0) and 25.8±7.8 m^2/s (K_H) above savanna, respectively. These values were calculated for all low level legs performed under 150m, and averaged over similar ecosystem. Two values only are available for K_H and z_0 : one for the savanna (including savanna 1, 2, and transitional woodland), one for the forest (including secondary and primary forest).

The parameter d is taken into account only above forest, which is typically composed of a continuous 35m canopy, with emergent trees reaching 60m, and consequently, d=35m. Above savanna, d=0.

As K_H has been averaged, equation (9) simplifies, giving r_a = 7 s/m above savanna 1 (z_M = 185m), 5.8 s/m above savanna 2 (z_M = 155m in average), 3.4 s/m above transitional woodlands (z_M = 90m), and 3.7 s/m above forest (z_M = 127m in average).

The calculation of r_b for rough ecosystems is taken from *Lagouarde et al.* [1993]:

$$r_b = \frac{3}{k u_*}\left(\frac{Sc}{Pr}\right)^{2/3} \quad (10)$$

where k=0.4 is the Von Karman constant, u_* is the friction velocity (0.355 m/s above forest, 0.376 m/s above savanna during EXPRESSO [*Delon et al.*, 2000]), Sc=1.07 is the Schmidt number for ozone, and Pr=0.72 is the Prandtl number. This leads to large values of r_b, 25.9 s/m above savanna and 27.5 s/m above forest.

The resistance r_c can be deduced from equation (8), and we found r_c = 205 s/m over savanna 1 (V_d = 0.0042 m/s), r_c = 101 s/m over savanna 2 (V_d = 0.0075 m/s in average), r_c = 71 s/m over transitional woodlands (V_d = 0.0100 m/s), and r_c = 35 s/m over forest (V_d = 0.0150 m/s in average).

These results allow the conclusion that the evolution of the deposition velocity mainly depends of surface resistance r_c (including explicit dependence of LAI), and that the aerodynamic resistance r_a does not significantly influence the deposition velocity over the forest.

These results suggest that V_d could be extrapolated over a whole latitudinal band, since the vegetation in Africa is distributed uniformly in latitude (Figure 7). In other words, the estimation of the LAI at a given point could give an order of magnitude of V_d, across the African continent. Of course, this is only valid when the aerodynamic resistance is low, and in the case of homogeneous surfaces on the same latitudinal band. Furthermore, the forest LAI does not vary throughout the year, whereas it decreases in the savanna at the height of fire season. We can assume that relation 7 is valid from April to December, and that it can be applied only in those individual cases.

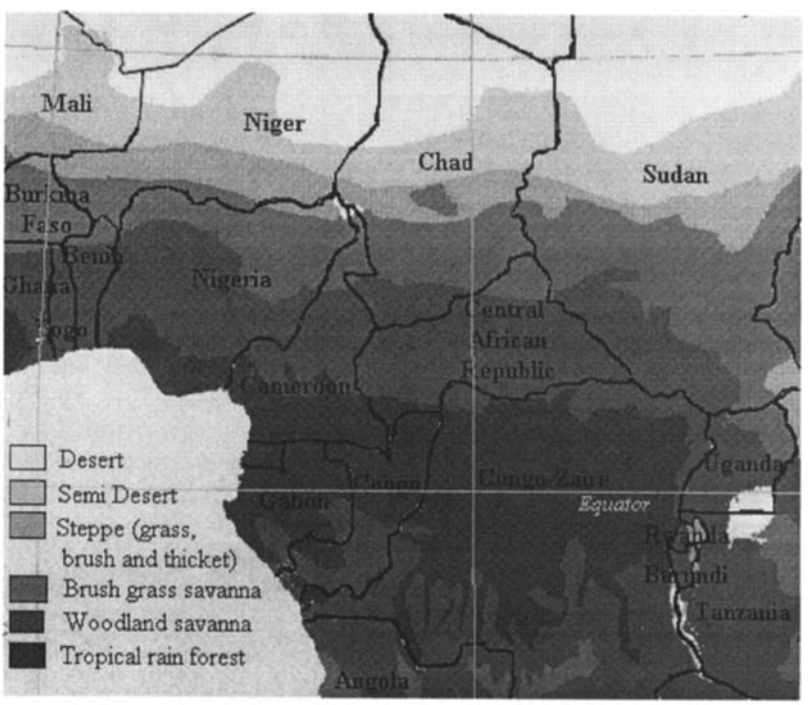

Figure 7. Latitudinal distribution of African vegetation.

4. Ozone Budget in the ABL Over Tropical Rain Forest

To analyze the ABL ozone budget over the tropical rain forest of the EXPRESSO area, a slab model proposed by *Lenschow et al.* [1981] is used. In this model the ozone rate of change with time $\partial[\overline{O_3}]/\partial t$ is balanced by mean horizontal advection $\overline{U}\,\partial[\overline{O_3}]/\partial x$, vertical flux divergence $\partial(\overline{w'O_3'})/\partial z$, and photochemical production $P(O_3)$ and/or loss $L(O_3)$ of ozone within the same volume:

$$\frac{\partial[\overline{O_3}]}{\partial t} = P(O_3) - L(O_3) - \overline{U}\frac{\partial[\overline{O_3}]}{\partial x} - \frac{\partial\left(\overline{w'O_3'}\right)}{\partial z}. \quad (11)$$

Because of flight constraints, the vertical profiles used for the estimation of ozone change were not performed over the same location. However, this is not a critical point for reactive compounds such as ozone, since the Congo rain forest basin over which it was measured is a homogeneous area. Above the forest the time derivative was estimated in the lowest part of the ABL from mean values of ozone mixing ratios. The lowest part of the ABL is generally well-mixed and does not show high ozone variations, compared with the HL above. If we take the example of flight 50, where the ozone increase was particularly easy to calculate, we can estimate the vertical flux divergence without difficulty. In the HL a net ozone production of 19 ppbv/h was estimated from the two profiles, the time difference between the two profiles being half an hour (Figure 8). A regular increase of $[O_3]$ is also found on the leg performed between the two profiles of flight 50 (the leg was performed in the HL). This ozone increase corresponds to an ozone production of about 10.5 ppbv/h in the HL, far lower than the 19 ppbv/h calculated from the profiles. The difference is attributed to advection, which plays an important role in the HL.

In the ABL the problem is different, and advection can be neglected. CO is used as a reference to evaluate the influence of the advection in the ABL because it can be considered as an inert tracer on the time scales and space scales of the campaign. Figure 9 shows that there is no CO increase from the beginning to the end of a leg performed in the ABL (750 m). The low CO variation allows the conclusion that CO is not advected from the north in this layer. If we assume a similar origin for CO and ozone precursors, we can say that the impact of horizontal advection is negligible on the ozone temporal variation in the ABL. Moreover, the ozone increase calculated on the leg is 9.2 ppbv/h, compared with 9.96 ppbv/h from the profiles performed before and after this leg. This adds support to the assumption that advection is negligible for ozone production in the ABL.

The vertical flux divergence can be approximated by the difference between the flux across the top of the ABL (Φ_{HL}) and the surface flux (Φ_S), divided by the ABL thickness Z_i. Advection is neglected, and the net rate of ozone change in the ABL over the forest becomes:

$$\frac{\partial[\overline{O_3}]}{\partial t} = P(O_3) - L(O_3) - \frac{(\Phi_{HL} - \Phi_S)}{Z_i} \quad (12)$$

The vertical ozone flux at the top of the ABL Φ_{HL} results from entrainment of air from the HL into the ABL, and is given by

$$\Phi_{HL} = \left(\overline{w'O_3'}\right)_{Z_i} = -V_e\Delta[O_3]$$

where V_e is the entrainment velocity and $\Delta[O_3]$ is the ozone mixing ratio change across the top of the ABL. The lifetime of ozone, which is around 2 days, allows the assumption that V_e is independent of chemical species, and that it can be calculated from the vertical transport of water vapor across the top of the ABL:

$$V_e = \frac{\overline{w'q'}}{\Delta q} = \frac{LE}{\rho L \Delta q} \quad (13)$$

where $LE = \rho L\overline{w'q'}$ is the latent heat flux (W/m^2), ρ is the air density, L is the latent heat of water vaporization, q' is the water vapor mixing ratio fluctuation, and Δq is the jump of water vapor mixing ratio between layers situated just below and just above the top of the ABL. The water vapor mixing ratio (measured on the boom of the aircraft) is first calculated at each level, then Δq is evaluated across the top of the ABL [*Delon et al.*, 2000].

The values of V_e and corresponding Φ_{HL} are given in Table 4. During the dry season over rain forest, the input of ozone from the HL around noon is higher than the ozone deposition,

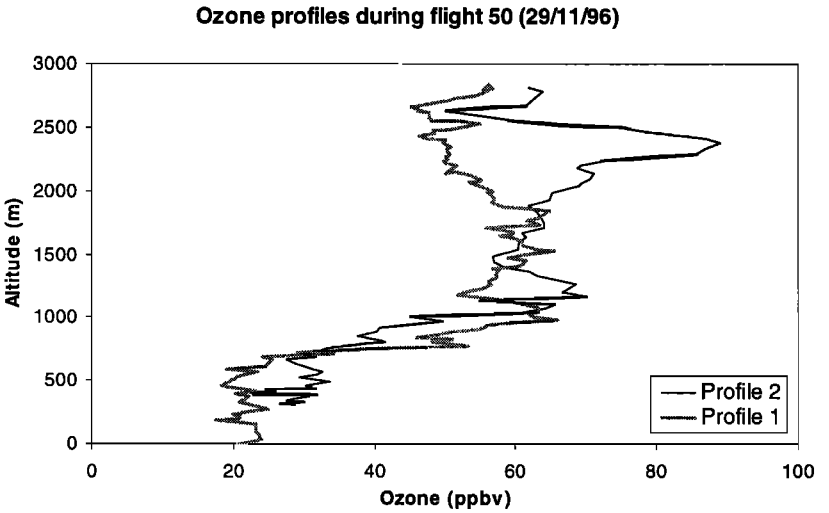

Figure 8. Vertical profiles of ozone obtained on November 29, 1996 (flight 50), just before the Bomassa forest (profile 1) and over the Bomassa forest (profile 2).

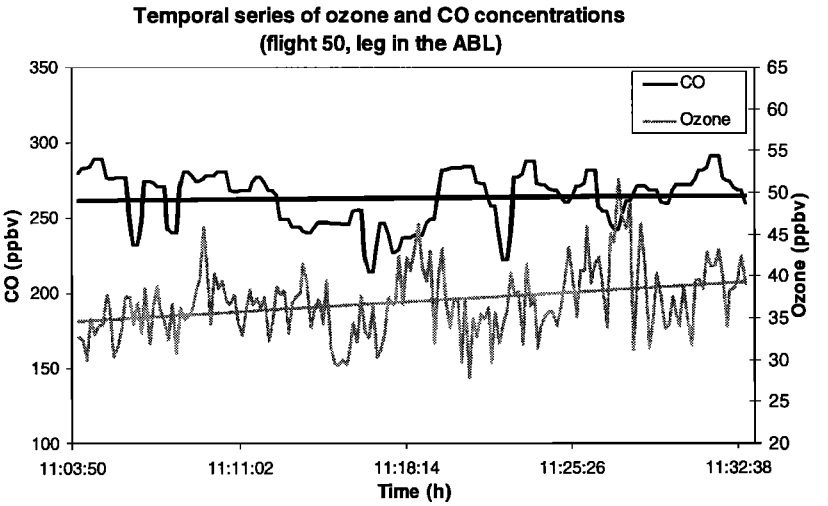

Figure 9. Evolution of [CO] (ppbv) and [O_3] (ppbv) at a constant altitude in the ABL between profiles 1 and profiles 2 of flight 50. Grey and black lines give the linear regression of temporal evolutions of ozone and CO concentrations, respectively.

on average -0.648 ppbv m/s compared with -0.350 ppbv m/s, corresponding to a net ozone downward vertical transport of about 1.2 ppbv/h in the ABL (the ABL thickness above forest is 925m in average). Over savanna, entrainment and surface fluxes are lower and the net vertical transport is only 0.5 ppbv/h.

Average net O_3 production $P'(O_3) = \{P(O_3) - L(O_3)\}$ can be compared to that calculated from the photo-stationary state (PSS) of NO_x and ozone:

$$P'(O_3) = J_{NO2} .[NO_2] - k [NO].[O_3]. \quad (14)$$

The photolysis rate J_{NO2} and the NO_2 and NO concentrations were measured on board during each flight [*Marion et al.*, 2000]. The kinetic constant used for the reaction $NO + O_3$ was $k = 1.8x10^{-12} \exp(-1370/T)$ [*Atkinson et al.*, 1992]. As an example, $P'(O_3)$ calculated for flight 50 is 15.5 ± 2.8 ppbv/h (Table 5).

O_3 production rates from PSS are higher than the values obtained from the net production (Table 5), possibly because of high values of [NO_2] and high [NO_2]/[NO] ratios *[Marion et al.*, 2000] . NO_2 could be formed from oxidation of NO by peroxy radicals, abundant in the tropical lower troposphere [*Hough*, 1991]. Nonetheless, the PSS is likely to overpredict the O_3 production since it represents the total NO to NO_2 conversion, including different reactions from $NO + O_3 \rightarrow NO_2 + O_2$ [*Kramp and Volz-Thomas*, 1997]. However, a quasi-balanced ozone budget can be found in some cases. Flight 52 for example, (performed above forest on December 1, 1996) is a good illustration of nearly steady state conditions (Table 5).

The ozone budget is also strongly influenced by photochemistry processes, remaining the most important mechanism for ozone production over the tropical forest during the fire period.

Indeed, high concentrations of NO_x (1.4 to 2.2 ppbv) were observed in the forest ABL (*Marion et al.*, 2000) during EXPRESSO (Figure 10, flight 50 is an example of high NO concentrations), and can be compared to values found in a nearby site during the DECAFE experiment in February 1988 (1.6 to 2 ppbv) [*Cros et al.*, 1992b].

Quite uniform NO_x (= $NO+NO_2$) levels in the ABL characterize homogeneous NO_x sources, and NO_x/NO_y ratios close to unity indicate that NO_x sources are close, where NO_y is the reactive odd nitrogen given by $NO_y = NO_x + \Sigma$ (nitrogen products of atmospheric oxidation). In the HL, the NO_x/NO_y ratio falls to 0.5 and NO_x concentrations are lower, characteristic of a photochemically older air mass. Nitrogen compounds in the ABL are for the most part emitted from soils and/or developed in the ABL, and downward transport from the HL is small. Accordingly, the high ozone production observed above the forest around noon (Figure 8) cannot be accounted for vertical transport alone but must be

Table 4. Entrainment Velocity V_e between HL and ABL, and Corresponding Ozone Flux Φ_{HL} at the Top of the ABL (i.e., at Z_i)[a]

Flight	Zone	Zi, m	$\Delta[O_3]$, ppbv	$\overline{V_e}$, cm/s	Φ_{HL} ppbv m/s	Φ_S ppbv m/s
46	F	800	36	-2.07	-0.745	-0.342
47	F	900	47	-0.88	-0.414	-0.262
50	F	1000	31	-2.47	-0.766	nd
52	F	1000	28	-2.38	-0.666	-0.508
Average		925		-1.95	-0.648	-0.350[b]
48	S1	1060	1060	-1.56	-0.250	-0.115

[a] Φ_S is the flux at the surface. F stands for rain forest, and S_1 is savanna 1. Here, nd is non determined.
[b] Averaged for all flights over forest.

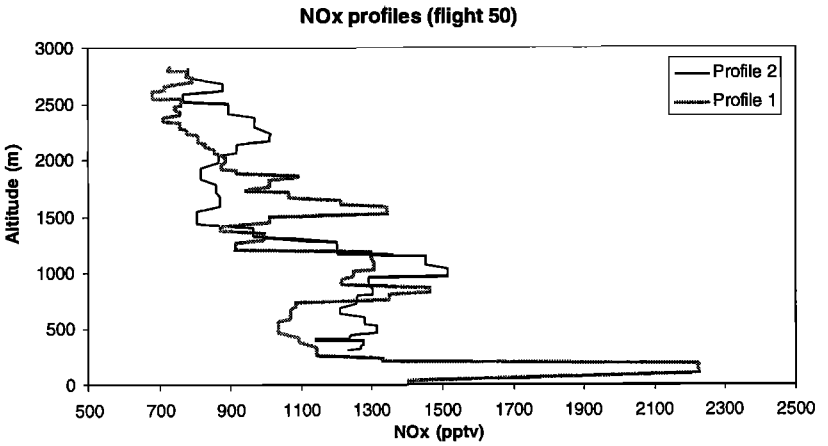

Figure 10. Ozone (ppbv) and NO_x (pptv) profiles for profile 2 of flight 50.

significantly influenced by photochemical production from biogenic precursors, which may accumulate during the night and in the early morning [*Cros et al*, 1992a; *Marion*, 1998] and/or from fire effluents. Thus ozone profiles suggest that photochemical production and vertical transport are largely stronger than deposition and other ozone sinks. However, high levels of primary combustion products (CO, condensation nuclei, NO_x) found in the forest ABL indicate a contamination by combustion products [*Delon et al.*, 2000]. This contamination decreases the ozone content in the forest ABL only if sources (fires) are close enough, since the ozone will be destroyed in reaction with strong and fresh concentrations of NO_x. The forest ABL may be contaminated by fires in the geographical transition zone, where the Harmattan flow competes with the Monsoon flow near the ground (transition between wet and dry seasons in the Northern Hemisphere). Moreover, scarce forest fires were detected by satellites during the campaign [*Grégoire et al.*, 1999].

High concentrations of ozone precursors suggest in part that photochemistry is the most important process for the ozone formation in the forest ABL. The contribution of entrainment processes at the top of the ABL, involving inlets of enriched ozone air masses in the ABL, is also consequent.

5. Summary and Conclusions

The EXPRESSO campaign took place in central Africa in November and December 1996 at the beginning of the dry season. Meteorological features of the studied zone were influenced by the proximity of the ITCZ, located at 5°-6°N at the end of the campaign. The chemical composition of the atmosphere was influenced by biomass burning, occurring mainly in the north of the EXPRESSO zone. Turbulent ozone fluxes were measured over savanna and rain forest with an aircraft designed to study turbulent processes in the first 4 km of the atmosphere. Deposition velocities were deduced from surface ozone fluxes. They increase from the savanna to the forest: ozone fluxes range from -0.12 to -0.38 ppbv m/s, and deposition velocities range from 0.4 to 1.5 cm/s. Around noon (time of the measurements) we observe a positive gradient between savanna and forest surface fluxes, and an approximately linear relation between deposition velocity and LAI This relation highlights the role of vegetation cover and surface resistance. For a known LAI a latitudinally constant structure of V_d was suggested by this linear relation, assuming that the vegetation is distributed in linear bands on the African continent and that r_a is small.

Ozone deposition was largely dominated by transport from above as indicated by high entrainment fluxes at the top of the ABL. The contribution of advection in the HL and in the ABL is estimated from aircraft legs and profiles, which show that the role of advection is negligible in the ozone budget. NO emission rates were measured in the experimental zone by *Serça et al.* [1994], and indicate that the forest is an O_3 sink. Indeed, tropical forest soils could provide large inputs of odd nitrogen species to the atmosphere, which may be important for global atmospheric chemistry [*Kaplan et al.*, 1988]. Above the EXPRESSO rain forest, around noon, ozone is produced through photochemical reactions, involving fresh precursors coming from forest soils and sometimes from nearby fires. High concentrations of ozone precursors in the ABL give an explanation to the fact that the photochemical production over the canopy is the dominant contribution to the ozone budget in the forest ABL.

Table 5. Budget of Ozone Around Noon in the ABL Over Tropical Rain Forest in Central Africa [a]

Flight	Net Production	Photochemistry Production	Dry Deposition	Entrainment
46	nd	24.4	1.4	2.1
47	9.6	19.0	1.0	1.6
50	10.0	15.5	1.4[b]	3.0
52	17.7	14.7	1.8	2.4

[a] Units are in ppbv/h.
[b] Mean surface flux is taken for the calculation of the dry deposition.

Acknowledgments. We thank the gouvernments of the Congo and CAR for the permission to conduct our investigation. We gratefully acknowledge the scientific and technical crew of the research aircraft ARAT. This research was supported by the Centre National de la Recherche Scientifique.

References

Affre, C., A. Carrara, J. Fontan, A. Druilhet, and A. Lopez, On turbulent flux of trace constituents measurements in the surface layer, Part I, Tests on vertical velocity stationarity, *Phys. Chem. Earth, 5-6*, 357-360, 1996.

Affre, C., A. Carrara, F. Lefebre, A. Druilhet, J. Fontan, and A. Lopez, Aircraft measurement of ozone turbulent flux in the atmospheric boundary layer, *Atmos. Environ., 33*, 1561-1574, 1999a.

Affre, C., A. Lopez, A. Carrara, A. Druilhet, and J. Fontan, The analysis of energy and ozone flux data from the LANDES 94 experiment, *Atmos. Environ., 34*, 803-821, 1999b.

Andreae, M.O., A. Chapuis, B. Cros, J. Fontan, G. Helas, C. Justice, Y.J. Kaufman, A. Minga, and D. Nganga, Ozone and Aitken nuclei over equatorial Africa: Airborne observations during DECAFE 88, *J. Geophys. Res., 97*, 6137-6148, 1992.

Atkinson, R., D.L. Baulch, R.A. Cox, R.F. Hampson Jr., J. A. Kerr, and J. Troe, Evaluated kinetic and photochemical data for atmospheric chemistry: Supplement IV, *J. Phys. Chem., Ref. Data, 21*, 1125-1568, 1992.

Cachier, H., and J. Ducret, Particulate carbon traces biomass burning influence in rains of Equatorial Africa, *Nature*, 352, 228-230, 1991.

Cahoon, D.R., Jr., B.J. Stocks, J.S. Levine, W.R. Coffer III, and K.P. O'Neill, Seasonal distribution of fires, *Nature*, 359, 813-815, 1992.

Carrara, A., Quantification et paramétrisation des flux d'ozone à l'interface végétation atmosphère : Application à un couvert forestier de résineux, Ph.D. thesis, Univ. Paul Sabatier, Toulouse, France, 1998.

Cieslik, S., and A. Labatut, Ozone and heat fluxes over a Mediterranean pseudosteppe, *Atmos. Environ., 31*, 177-184, 1997.

Cros, B., R. Delmas, D. Nganga, and B. Clairac, Seasonal trends of ozone in equatorial Africa: Experimental evidence of photochemical formation, *J. Geophys. Res., 93*, 8355-8366, 1988.

Cros, B., J. Fontan, A. Minga, G. Helas, D. Nganga, R. Delmas, A. Chapuis, B. Benech, A. Druilhet, and M.O. Andreae, Vertical profiles of ozone between 0 and 400 m in and above the African equatorial forest, *J. Geophys. Res., 97*, 12,877-12887, 1992a.

Cros, B., D. Nganga, A. Minga, J. Fishman, and V. Brackett, Distribution of tropospheric ozone at Brazzaville, Congo, determined from ozonesonde measurements, *J. Geophys. Res., 97*, 12,869-12,875, 1992b.

Cros, B., A. Brou, D. Orange, M. Dimbele, and J.P. Lacaux, Tropospheric ozone on both sides of the equator of Africa, in *Biomass Burning and Global Change*, edited by J.S. Levine, pp. 327-332, MIT Press, Cambridge, Mass., 1996.

Delmas R., et al., Experiment for Regional Sources and Sinks of Oxidants (EXPRESSO): An overview, *J. Geophys. Res., 104*, 30,609-30,624, 1999.

Delon, C., A. Druilhet, R. Delmas, and P. Durand, Dynamic and thermodynamic structure of the lower troposphere above rain forest and wet savanna during the EXPRESSO campaign, *J. Geophys. Res., 105*, 14,823-14,840, 2000.

Fan, S. M., S.C. Wofsy, P.S. Backwin, D.J. Jacob, and D.R. Fitzarrald, Atmosphere-biosphere exchange of CO_2 and O_3 in the central Amazon forest, *J. Geophys. Res., 95*, 16,851-16,864, 1990.

Fishman, J., P. Minnis, and H.G. Reichle Jr., The use of satellite data to study tropospheric ozone in the tropics, *J. Geophys. Res., 91*, 14,451-14,465, 1986.

Fishman, J., C. E. Watson, J.C. Larsen, and J.A. Logan, Distribution of tropospheric ozone determined from satellite data. *J. Geophys. Res., 95*, 3599-3617, 1990.

Fishman, J., K. Fakhruzzaman, B. Cros, and D. Nganga, Identification of widespread pollution in the southern hemisphere deduced from satellite analyses, *Science, 252*, 1693-1696, 1991.

Fishman, J., V. G. Brackett, and K. Fakhruzzaman, Distribution of tropospheric ozone in the tropics from satellite and ozone measurements, *J. Atmos. Terr. Phys., 54*, 589-597, 1992.

Fishman, J., V.G. Brackett, E.V. Browell, and W. B. Grant, Tropospheric ozone derived from TOMS/SBUV measurements during TRACE-A, *J. Geophys. Res., 101*, 24,069-24,082, 1996.

Grégoire, J.M., and S. Pinnock, Satellite monitoring of vegetation fires for EXPRESSO: Outline of activity and relative importance of the study area in the global picture of biomass burning, *J. Geophys. Res. 104*, 30,691-30,700, 1999.

Günsten, H., and G. Heinrich, On line measurements of ozone surface fluxes, part I, Methodology and instrumentation, *Atmos. Environ., 30*, 897-909, 1996.

Günsten, H., G. Heinrich, R.W.H. Schmidt, and U. Schurath, A novel ozone sensor for direct eddy flux measurements. *J. Atmos. Chem., 14*, 73-84, 1992.

Hough, A.M., Development of a global tropospheric model: Model chemistry, *J. Geophys. Res., 96*, 7325-7362, 1991.

Kaplan, W.A., S.C. Wofsy, M. Keller, and J.M. Da Costa, Emission of NO and deposition of O_3 in a tropical forest system, *J. Geophys. Res., 93*, 1389-1395, 1988.

Klinger, L.F., J. Greenberg, A. Guenther, G. Tyndall, P. Zimmerman, M. M'Bangui, J.M. Motsamboté, and D. Kenfack, Patterns in volatile organic compound emissions along a savanna-rain forest gradient in central Africa, *J. Geophys. Res., 103*, 1443-1454, 1998.

Kramp, F., and A. Volz-Thomas, On the budget of OH radicals and ozone in an urban plume from the decay of C5-C8 hydrocarbons and NO_x, *J. Atmos. Chem., 28*, 263-282, 1997.

Lacaux, J.P., R. Delmas, C. Jambert, and T.A.J. Kuhlbusch, NO_x emissions from African savanna fires, *J. Geophys. Res., 101*, 23,585 -23,595, 1996.

Lagouarde, J.P., Y. Brunet, and R.G.B. André, A simple PBL approach for estimating actuel evapotranspiration from TIR data over a pine forest canopy, paper presented at the Workshop on Thermal Remote Sensing of the Energy and Water Balance Over Vegetation in Cunjunction With Other Sensors, Penn State Univ./CEMAGREF/CRPE, La Londe Les Maures, France, Sept. 20-23, 1993.

Lefeivre, B., Etude expérimentale et par modélisation des caractéristiques physiques et chimiques des précipitations collectées en forêt équatoriale africaine, PhD thesis, 206 pp., Univ. Paul Sabatier, Toulouse, France, 1993.

Lenschow, D. H., R. Pearson, and B.B. Stankov, Estimating the ozone budget in the boundary layer by use of aircraft measurements of ozone eddy flux and mean concentration, *J. Geophys. Res., 86*, 7291-7297, 1981.

Leroux, M., Le climat de l'Afrique tropicale, PhD thesis, 1427 pp., Univ. De Dakar, Dakar, Sénégal, 1980.

Marion, T., Mesures aéroportées des oxydes d'azote: Application à l'étude des processus de production dans l'atmosphère tropicale, Ph.D. thesis, Univ. Paris XII, Créteil, France, 1998.

Marion, T., P.E. Perros, R. Losno, and F. Steiner, Ozone production efficiency in savanna and forested areas during the EXPRESSO experiment, J. Atmos. Chem., in press, 2000.

Marenco, A., J.C. Medale, and S. Prieur, Study of tropospheric ozone in the tropical belt (Africa, America) from STRATOZ and TROPOZ campaigns, *Atmos. Environ., Part A, 24*, 2823-2834, 1990.

Serça, D., R. Delmas, C. Jambert, and L. Labroue, Emissions of nitrogen oxides from equatorial rain forest in central Africa: Origin and regulation of NO emissions from soils, *Tellus, Ser. B, 46*, 243-254, 1994.

Webb, E. K., G.I. Pearman, and R. Leuning. Correction of flux measurements for density effects due to heat and vapor transfer, *Q. J. R. Meteorol. Soc., 106*, 85-100, 1980.

Weseley, M.L., J.A. Eastman, D.H. Stedman, and E.D. Yalvae, An eddy-correlation measurement of NO_2 flux to vegetation and comparison to O_3 flux, *Atmos. Environ., 16*, 815-820, 1982.

C. Affre, B. Cros (corresponding author), C. Delon, A. Druilhet, and A. Lopez, Laboratoire d'Aérologie, Unité Mixte de Recherche 5560, Centre National de la Recherche Scientifique/Université Paul Sabatier, Observatoire Midi Pyrénées, 14 av. E. Belin, 31400 Toulouse, France. (crob@aero.obs-mip.fr)

T. Marion and P.E. Perros, Laboratoire Interuniversitaire des Systèmes Atmosphériques, Unité Mixte de Recherche 7583, Centre National de la Recherche Scientifique/Université Paris 12, 61 av. du Général de Gaulle, 94010 Créteil Cedex, France.

(Received April 11, 2000; revised July 13, 2000; accepted July 20, 2000.)